

# Error tolerance in an NMR implementation of Grover's fixed-point quantum search algorithm

Li Xiao and Jonathan A. Jones\*

Centre for Quantum Computation, Clarendon Laboratory, University of Oxford, Parks Road, OX1 3PU, United Kingdom

(Received 8 April 2005; published 22 September 2005)

We describe an implementation of Grover's fixed-point quantum search algorithm on a nuclear magnetic resonance quantum computer, searching for either one or two matching items in an unsorted database of four items. In this algorithm the target state (an equally weighted superposition of the matching states) is a fixed point of the recursive search operator, so that the algorithm always moves towards the desired state. The effects of systematic errors in the implementation are briefly explored.

DOI: 10.1103/PhysRevA.72.032326

PACS number(s): 03.67.Lx, 82.56.-b

## I. INTRODUCTION

Grover's quantum search [1,2] is one of the key algorithms in quantum computation [3], allowing an unstructured database to be searched more efficiently than can be achieved by any classical algorithm. It is most simply described in terms of a binary function  $f$ , with an  $n$ -bit input register, permitting  $N=2^n$  inputs, and a single output bit. This function has the value of 1 for  $k$  desired (*matching* or *satisfying*) inputs and zero for the other  $N-k$  inputs, and can only be investigated by an oracle that returns the value for any desired input. Grover's original algorithm uses a quantum oracle that performs the transformation

$$|x\rangle \rightarrow (-1)^{f(x)}|x\rangle, \quad (1)$$

which is applied alternately with an amplitude amplification operator. Beginning from the state  $H_n|\mathbf{0}\rangle$ , where  $H_n$  is the  $n$ -qubit Hadamard and  $|j\rangle$  indicates an  $n$ -qubit quantum register containing the number  $j$ , the system is rotated towards an equally weighted superposition of the satisfying inputs. A measurement of the register after  $O(\sqrt{N/k})$  steps will return one of the satisfying inputs with high probability, while a classical search will take  $O(N/k)$  queries on average.

Grover's search is known to be optimal [4] when the number of matching inputs is known, but problems occur when  $k$  is unknown. As the basic procedure is a rotation, once the desired state is reached further iterations will drive the system *away* from this state. Thus it is necessary either to estimate the value of  $k$  (for example, by approximate quantum counting [5,6]) or to use an algorithm which is more robust to errors in the value of  $k$ .

Recently, Grover has described a quantum algorithm [7] that overcomes this problem by driving the system asymptotically towards the desired state: the algorithm will always move towards the target and cannot overshoot. This might seem impossible, as unitarity means that any iterative algorithm cannot have a fixed point, but the algorithm overcomes this by using a process that is recursive rather than iterative, so that the target state can act as a fixed point. A further

consequence of the fixed-point behavior is that the algorithm should be relatively robust to certain types of systematic error in its implementation.

## II. THEORY

Grover's algorithm comes in many forms [2], and here we describe just one of these, before relating it to the newer algorithm [7]. Consider the transformation

$$UR_0U^\dagger R_f U|\mathbf{0}\rangle, \quad (2)$$

where  $R_f$  is a phase oracle that applies a phase of  $\phi$  to all basis states satisfying the function  $f$  and  $R_0$  applies this phase shift to the initial state  $|\mathbf{0}\rangle$ . If we take  $U=H_n$  and  $\phi=\pi$ , then this corresponds to the first iteration of the original Grover algorithm. Subsequent steps are obtained by applying the last four operations  $r$  times, thus applying successive rotations. Larger rotations can be defined using a recursive approach, by taking

$$V_{r+1} = V_r R_0 V_r^\dagger R_f V_r \quad (3)$$

with  $V_0=U$ . For the original search algorithm  $U^\dagger=U$  and  $R^\dagger=R$ , so that each recursive operator simply corresponds to one of the iterative operators.

Grover's fixed point quantum search differs significantly from this by choosing  $\phi=\pi/3$ , so that  $R^\dagger$  does not equal  $R$ . Thus, the recursive operators are not simply iterative, and have to be worked out separately for each value of  $r$ ; for more details see the original paper [7]. Here we consider the case of  $n=2$ , with either  $k=1$  or  $k=2$ , and take  $U$  as the pseudo-Hadamard gate (a  $90_y^\circ$  rotation), as these are the examples we implement experimentally.

For the case of  $k=1$  there is a single satisfying input  $|s\rangle$ . The probability of the algorithm succeeding depends on the projection of the final state onto the satisfying input and is given by

$$P_r = |\langle s|V_r|\mathbf{00}\rangle|^2, \quad (4)$$

which simplifies to

$$P_r = 1 - (3/4)^{3^r}. \quad (5)$$

Clearly this converges rapidly to 1, as shown by the numerical values listed in Table I. For the case  $k=2$  the target state

\*Electronic address: jonathan.jones@qubit.org

TABLE I. Success probabilities ( $P_r$ ) and the total number of queries used ( $Q_r$ ) for the  $r$ th stage of Grover's fixed-point quantum search algorithm with  $n=2$ ; for more details see the main text.

$r$	$P_r(k=1)$	$P_r(k=2)$	$Q_r$
0	0.2500	0.5000	0
1	0.5781	0.8750	1
2	0.9249	0.9980	4
3	0.9996	1.0000	13
4	1.0000	1.0000	40

is an equally weighted superposition of the two satisfying states, and the success probability is given by

$$P_r = 1 - (1/2)^{3^r}, \quad (6)$$

which rises even more rapidly.

Note, however, that  $r$  is the order of the recursive operator and not the number of queries, which is given by  $Q_r = (3^r - 1)/2$ . This query count, which is also listed in Table I, also rises rapidly with  $r$ , so that the fixed-point algorithm is less efficient than a traditional Grover search when the value of  $k$  is known. This is unsurprising, as the traditional search is known to be optimal [4] in this case! When the value of  $k$  is unknown, however, the current algorithm outperforms previously known methods, as described by Grover [7]. It is also relatively robust against experimental errors, as discussed below.

### III. EXPERIMENT

This algorithm was implemented on a two-qubit nuclear magnetic resonance (NMR) quantum computer [8–13], searching for either one or two satisfying inputs for a function with four inputs. The spin system chosen was formed by the  $^1\text{H}$  and  $^{13}\text{C}$  nuclei in a sample of 10 mg of  $^{13}\text{C}$  labeled sodium formate ( $\text{Na}^+\text{HCO}_2^-$ ) dissolved in 0.75 ml of  $\text{D}_2\text{O}$  at a temperature of 20 °C.

All experiments were performed on a Varian Unity Inova spectrometer with a nominal  $^1\text{H}$  frequency of 600 MHz. The  $^1\text{H}$  and  $^{13}\text{C}$  frequencies were adjusted to be in exact resonance with the respective nuclei so that the spin Hamiltonian in the rotating frame, written using Product Operator notation [14], is given by the Ising coupling as

$$\mathcal{H} = \pi J 2H_z C_z \quad (7)$$

with  $J=194.8$  Hz. The measured relaxation times were  $T_1^{\text{H}}=6.5$  s,  $T_2^{\text{H}}=1.2$  s,  $T_1^{\text{C}}=16$  s, and  $T_2^{\text{C}}=0.6$  s. A repetition delay of 120 s was used in all experiments; this is more than seven times the longest  $T_1$  so that saturation effects can be ignored. The rf pulse powers were adjusted so that a  $90^\circ$  rotation took 15  $\mu\text{s}$  for both spins.

The current search algorithm requires the implementation of  $U$  gates and  $R$  gates, as well as the inverse operations. The  $U$  gates were implemented as simultaneous  $90_y^\circ$  pulses, while the  $R$  gates were decomposed into periods of evolution under the Ising coupling and composite  $z$  rotations [15], con-

structed from  $x$  and  $y$  pulses.  $R_f$  gates were implemented for each of the four functions  $f$  with  $k=1$  and the six functions with  $k=2$ ; note that the  $R_0$  gate is identical to  $R_f$  for the function with  $|00\rangle$  as the single satisfying input. Each gate was locally optimized by combining pulses, but no optimization across gates was performed. To explore the effects of systematic errors, experiments were performed using both naive rf pulses and BB1 composite pulses [16,17] that correct for systematic errors in pulse lengths arising from rf inhomogeneity.

A pseudopure initial  $|00\rangle$  state was prepared by spatial averaging [12]. Experiments were performed for each of the functions with  $k=1$  and  $k=2$ , with the order  $r$  of the recursive search operator taking the values  $r=0,1,2,3$ . The  $r \rightarrow \infty$  limit was simulated by directly transforming the initial state into the desired target state. The state of the spin system was then probed to obtain information on the performance of the algorithm.

For the case of  $k=1$ , the target state is a single eigenstate and the analysis is simple. A crush gradient was applied to dephase any off-diagonal error terms in the density matrix [18] and the  $^1\text{H}$  NMR spectrum was observed after a  $90_y^\circ$   $^1\text{H}$  pulse. The state of the first qubit, stored on the  $^1\text{H}$  nucleus, is then encoded in the sign of the NMR resonance, and the state of the second qubit, stored on the  $^{13}\text{C}$  nucleus, is revealed, by which of the two components of the  $^1\text{H}$  multiplet are observed. For more details see [12]. Note that this approach is only practical in systems with relatively small numbers of qubits, and in large spin systems it would be necessary to measure all the spin states directly.

Finally, the success probability  $P_r$  of the algorithm can be estimated from the intensity of the NMR spectrum compared with a reference spectrum [19]. Because NMR experiments are only sensitive to the traceless part of the density matrix the observed signal strength is not directly proportional to  $P_r$ , but rather to the fractional signal  $F_r$ , which is given by  $F_r = (4P_r - 1)/3$ . In particular, no signal is expected for the case  $P_r = 1/4$ .

For the case of  $k=2$  the situation is slightly more complicated, as the target state is a superposition of the two matching states, but we chose to analyze the data in the same way. For four of the six functions this results in a  $^1\text{H}$  NMR spectrum containing *both* components of the multiplet, with the result encoded in the signs of these two lines, while for the other two functions no signal is expected. For the four functions giving rise to visible signals the success probability and fractional signal are related by  $F_r = 2P_r - 1$ , so that no signal is expected for the case  $P_r = 1/2$ .

### IV. RESULTS

We began by implementing the four functions with  $k=1$  using naive rf pulses, with the results shown in Fig. 1. The spectra all have the form expected, showing one major component in each multiplet. A positive line indicates that the first qubit is in state  $|0\rangle$ , while a negative line indicates state  $|1\rangle$ . A signal in the left-hand component indicates that the second qubit is in state  $|0\rangle$ , while the right-hand component indicates state  $|1\rangle$ . The minor signals visible on the other

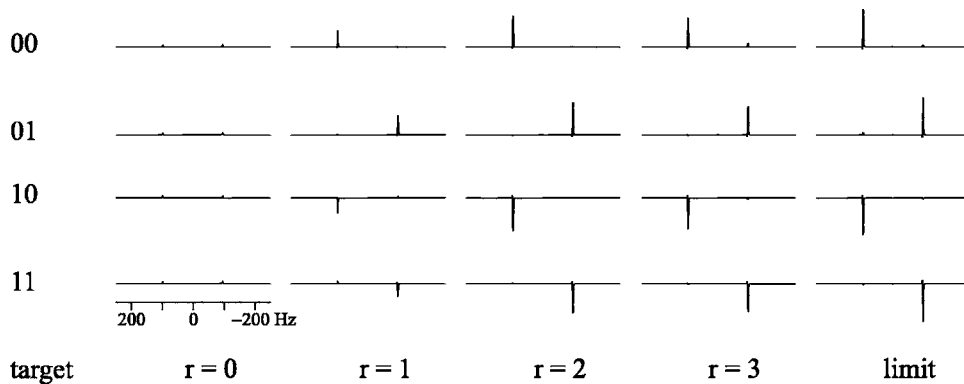


FIG. 1. Experimental  $^1\text{H}$  NMR spectra from an implementation of Grover's fixed-point quantum search algorithm on a two-qubit NMR quantum computer with one matching state. For a description of the readout scheme see the main text. Spectra are shown for the cases  $r=0, 1, 2, 3$ , and a simulation of the  $r \rightarrow \infty$  limit was obtained by directly transforming the initial state into the target state. Spectra are plotted using NMR conventions, with frequency (measured by the offset from the rf frequency) increasing from right to left. A horizontal axis is plotted below the bottom left spectrum and can be applied to all spectra. The vertical scale is arbitrary, but the same for all spectra.

component of each multiplet, as well as the minor phase distortions visible in some spectra, can be ascribed to errors in the implementation.

As expected, the signal intensity initially rises towards the limiting value, although it seems to fall slightly at  $r=3$ . This point is explored in more detail in Fig. 2, which compares the integrated intensity of the largest component with the theoretically expected values. Initially the experimental data points lie quite close to the theoretical line, but for  $r=3$  the match is much less good. We originally ascribed this to the effects of errors in the pulse sequence, and in particular to the cumulative effects of pulse length errors, and sought to reduce these effects by using BB1 composite pulses [16,17]. The outline results of this approach are also shown in Fig. 2 (raw data not shown).

While this approach did give slightly improved results for  $r \leq 2$  (especially for the case  $r=0$  where the search operator comprises a single  $90^\circ$  pulse), it does not remove the drop in intensity seen at  $r=3$ , which we now believe arises from

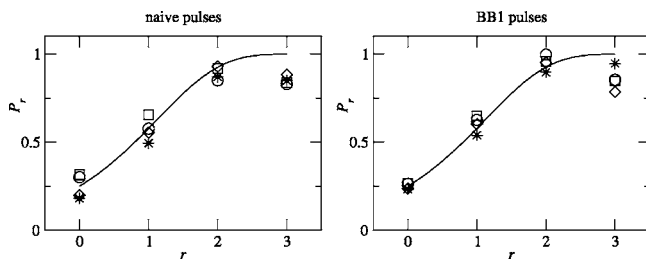


FIG. 2. Experimental success probability for the cases  $r=0, 1, 2, 3$  for the four possible functions with a single matching state. Results are shown for both simple single-qubit gates implemented by naive rf pulses and for BB1 composite pulses. Fractional intensities are obtained by comparing the spectral intensities with those in the spectra obtained by directly transforming the initial state into the target state, and these are converted to probabilities as described in the main text. The theoretical result is shown as a smooth curve even though it is strictly only defined for integer values of  $r$ ; experimental values are shown as squares, circles, diamonds, and stars for target states of  $|00\rangle$ ,  $|01\rangle$ ,  $|10\rangle$  and  $|11\rangle$ , respectively.

errors in the implementation of the  $R$  gates. The errors are different for the four different functions (the error arising from noise in the experimental spectra was estimated by repetition and is much smaller than the scatter observed), consistent with this suggestion.

The lack of improvement from the use of BB1 pulses may seem disappointing, but is in fact quite interesting in its own right. We have assumed that the  $U$  operator is implemented by a  $90^\circ_y$  pulse, but Grover's algorithm can be made to work with many different operators [2]. In combination with the fact that Grover's newer algorithm always moves towards the target state, this makes the algorithm intrinsically tolerant of pulse length errors [7]. In fact the experimental spectra observed are of remarkably high quality, given that the case of  $r=3$  corresponds to the implementation of 26 two-qubit gates (13 instances of  $R_f$  and 13 of  $R_0$ ) and around 200 rf pulses.

Finally we consider the situation when there are two matching states; that is,  $k=2$ . The search operators were implemented directly, rather than by applying two single-match operators in sequence, and are slightly simpler than for the case of a single target state (in some cases the function operators  $R_f$  do not require two qubit gates). There are six possible search operators  $R_f$ , all of which were implemented using both naive and BB1 composite pulses, but here we concentrate on two cases: firstly where the target states are  $|00\rangle$  and  $|01\rangle$  (giving a  $^1\text{H}$  spectrum with both components of the multiplet positive), and secondly where they are  $|10\rangle$  and  $|01\rangle$  (giving a spectrum with the left-hand component negative and the right-hand component positive).

The experimental results from these cases are summarized in Fig. 3, where the intensity of each spectrum was obtained using either the sum or the difference of the integrals of the two components as appropriate. We show results obtained using naive pulses, but as before the results with BB1 pulses were very similar. As before, the experimental data broadly follow the theoretical curve, and this time the results for  $r=2$  and  $r=3$  have almost the same intensity, as predicted by Table I. This slight improvement may reflect the fact that the  $R_f$  gates are slightly simpler for  $k=2$  than for  $k=1$ .

In principle, one could also study the cases of  $k=3$  and  $k=4$ , but these are not particularly interesting. There is a

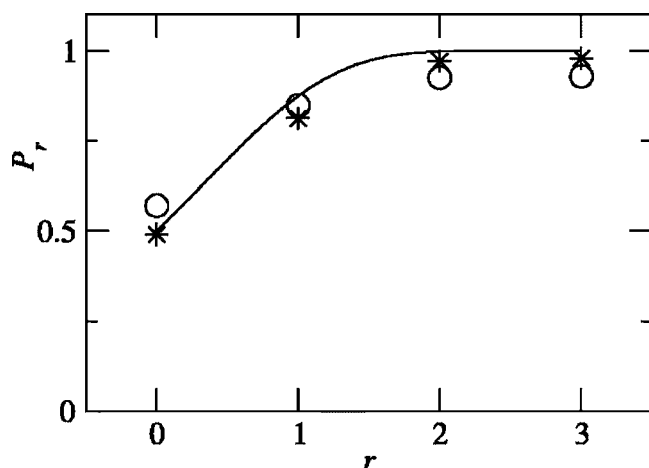


FIG. 3. Experimental success probability for the cases  $r = 0, 1, 2, 3$  for two of the six possible functions with two matching states. For further details see Fig. 2. Experimental values were obtained using naive pulses and are shown as circles for matching states of  $|00\rangle$  and  $|01\rangle$  and stars for matching states of  $|10\rangle$  and  $|01\rangle$ .

correspondence between the functions with  $k$  and those with  $N-k$  satisfying inputs, and for quantum oracles (controlled phase gates) the operators differ only by global phases. Thus the case of  $k=3$  is indistinguishable from that of  $k=1$ , as phase shifting three states in one direction is equivalent to shifting the fourth state in the opposite direction. The case of  $k=4$  is trivial, as applying phase shifts to all the states is

nothing more than a global phase, and thus the function operator corresponds to the identity operation.

## V. CONCLUSIONS

Our experimental results are broadly consistent with those predicted for an implementation of Grover's fixed-point quantum search algorithm. The observed success probability initially rises with the order of the (recursively defined) search operator, although a falloff is observed at  $r=3$ , which we ascribe to experimental errors in the operators  $R_f$  and  $R_0$ . Despite these experimental errors, the results are remarkably good given the complexity of the pulse sequences involved.

As predicted by Grover [7], the algorithm is remarkably robust to systematic errors which are equivalent for a gate and its inverse. This is largely true of the  $U$  gates, which are implemented using rf pulses, and the use of BB1 gates to correct systematic errors has little effect except in the case  $r=0$ . It is not true for the  $R$  gates, as our implementation of  $R^\dagger$  is somewhat different from that of  $R$ , and the errors in these two gates will not be equivalent.

This error-tolerance property can in principle be used to develop methods for more general correction of systematic errors [7], but we do not address this point here.

## ACKNOWLEDGMENTS

We thank the UK EPSRC and BBSRC for financial support.

- 
- [1] L. K. Grover, Phys. Rev. Lett. **79**, 325 (1997).
  - [2] L. K. Grover, Phys. Rev. Lett. **80**, 4329 (1998).
  - [3] C. H. Bennett and D. P. DiVincenzo, Nature (London) **404**, 247 (2000).
  - [4] C. Zalka, Phys. Rev. A **60**, 2746 (1999).
  - [5] M. Boyer, G. Brassard, P. Høyer, and A. Tapp, Fortschr. Phys. **46**, 493 (1998).
  - [6] J. A. Jones and M. Mosca, Phys. Rev. Lett. **83**, 1050 (1999).
  - [7] L. K. Grover, e-print quant-ph/0503205.
  - [8] D. G. Cory, A. F. Fahmy, and T. F. Havel, in *Proceedings of PhysComp '96* (New England Complex Systems Institute, Cambridge, MA, 1996).
  - [9] D. G. Cory, A. F. Fahmy, and T. F. Havel, Proc. Natl. Acad. Sci. U.S.A. **94**, 1634 (1997).
  - [10] N. A. Gershenfeld and I. L. Chuang, Science **275**, 350 (1997).
  - [11] J. A. Jones and M. Mosca, J. Chem. Phys. **109**, 1648 (1998).
  - [12] J. A. Jones, Prog. Nucl. Magn. Reson. Spectrosc. **38**, 325 (2001).
  - [13] L. M. K. Vanderspen and I. L. Chuang, Rev. Mod. Phys. **76**, 1037 (2004).
  - [14] O. W. Sørensen, G. W. Eich, M. H. Levitt, G. Bodenhausen, and R. R. Ernst, Prog. Nucl. Magn. Reson. Spectrosc. **16**, 163 (1983).
  - [15] R. Freeman, *Spin Choreography* (Spektrum, Oxford, 1997).
  - [16] S. Wimperis, J. Magn. Reson., Ser. A **109**, 221 (1994).
  - [17] H. K. Cummins, G. Llewellyn, and J. A. Jones, Phys. Rev. A **67**, 042308 (2003).
  - [18] J. A. Jones, M. Mosca, and R. H. Hansen, Nature (London) **393**, 344 (1998).
  - [19] M. S. Anwar, L. Xiao, A. J. Short, J. A. Jones, D. Blazina, S. B. Duckett, and H. A. Carteret, Phys. Rev. A **71**, 032327 (2005).